

Molecular beam epitaxy growth of $\text{Ge}_{1-y}\text{C}_y$ alloys on Si (100) with high carbon contents

K. J. Roe,^{a)} M. W. Dashiell, and J. Kolodzey

Department of Electrical and Computer Engineering, University of Delaware, Newark, Delaware 19716

P. Boucaud and J.-M. Lourtioz

Institut d'Electronique Fondamentale, Université Paris Sud, 91405 Orsay, France

(Received 30 October 1998; accepted 23 March 1999)

Group IV alloys are attracting strong interest for Si-based optoelectronics. The effects of C on the electrical and optical properties, however, are still not well understood, especially for high Ge content. In this report, we describe optical, structural, and compositional measurements of a series of thick, relaxed *p*-type $\text{Ge}_{1-y}\text{C}_y$ layers on *n*-type Si (100) substrates. The alloy layers were 0.5 μm thick and were grown by solid source molecular beam epitaxy at a substrate temperature of 300 °C and *p*-type doped with different B concentrations. X-ray diffraction indicated that the layers were single crystalline and nearly fully relaxed. The optical absorption was measured using a waveguide structure using Fourier transform infrared spectroscopy. The absorption data versus photon energy data fit indicated an indirect band gap, and one sample had a band gap of 774 meV compared to 660 meV for pure Ge. For single-crystalline, relaxed layers, the effect of C was to increase the band gap energy. These measurements show that alloying Ge with C provides a way to vary the optical absorption, which may be useful for device applications. © 1999 American Vacuum Society. [S0734-211X(99)07103-6]

Group IV alloys are attracting attention for use in Si-based optoelectronics. Optical and electrical devices use $\text{Si}_{1-x}\text{Ge}_x$ alloys to improve device performance compared to pure Si, and C may give new possibilities for devices. For example, it has been shown that the addition of C stabilizes the alloys by reducing strain and dopant out-diffusion.¹ Carbon has a low equilibrium solid solubility in Ge, so therefore a nonequilibrium growth technique such as molecular beam epitaxy (MBE) is necessary to achieve significant C concentrations. Metastable $\text{Ge}_{1-y}\text{C}_y$ alloys with carbon concentrations of $y \approx 0.01$ have been grown by MBE at low growth temperatures, near 400 °C.² Here we report on the growth, optical, and structural properties of crystalline $\text{Ge}_{1-y}\text{C}_y$ alloys with a range of C content.

The $\text{Ge}_{1-y}\text{C}_y$ alloys were grown by solid-source MBE in an EPI Model 620 system. The system features six effusion cells and a substrate introduction chamber. The typical base pressure of the system before growth was on the order of 10^{-11} Torr. During growth, the system pressure was typically 5×10^{-9} Torr, maintained by a liquid helium cooled cryopump.

The Ge beam was formed by thermally evaporating triple zone-refined intrinsic Ge in a pyrolytic boron nitride (PBN) crucible. To minimize boron contamination from the crucible, the cell temperature was kept below 1380 °C. At 1325 °C the Ge growth rate was approximately 0.2 Å/s.

The C beam was produced by an EPI single-filament carbon source. The beam is created by sublimating a pyrolytic graphite filament resistively heated by a direct current power supply. Typical current values were 48–50 A, resulting in an estimated filament temperature of 2300 °C.

Substrates were *p*-type (100)-oriented 3 in. diameter single crystal Si wafers with a resistivity of 1–10 Ωcm . Wafers were prepared by degreasing, etching in $\text{H}_2\text{O}:\text{H}_2\text{O}_2:\text{HCl}(5:3:3)$, and dipping in $\text{HF}:\text{H}_2\text{O}(1:10)$ to terminate the surface with H.³ Wafers were then immediately loaded into the MBE for growth. The substrate was then heated above 200 °C for 1 h to desorb any surface contaminants. The growth conditions for the samples are shown in Table I. Alloys were grown at a substrate temperature of 300 °C. Substrate temperature values of a nearby thermocouple were calibrated by the Si eutectic transition with Al and Au. Alloys were grown at low temperature in an attempt to maximize the substitutional C incorporation. The GeC layer was grown directly onto the Si substrate without any buffer layers. The aim was to grow thick relaxed films in order to study the bulk properties of unstrained layers, which were thick enough so that the interface dislocations would not adversely affect the measured parameters. Reflection high-energy electron diffraction (RHEED) analysis both during and after growth showed 2×1 surface reconstruction. Layer thicknesses were estimated from growth conditions and confirmed by Rutherford backscattering (RBS) to be 0.5 μm .

Optical absorption measurements were performed by Fourier transform infrared (FTIR) spectroscopy measurements. A waveguide reflection method was used to obtain approximately eight bounces through the alloy film.⁴ Figure 1 illustrates the waveguide reflection geometry. The samples were prepared to a size of 5 mm \times 8 mm and mechanically polished at a 45° angle at opposite ends. FTIR data from a pure Si waveguide reference was subtracted from the waveguide data to yield the absorption of the layers alone. This layer

^{a)}Electronic mail: roe@ee.udel.edu

TABLE I. MBE growth conditions for the GeC layers; the substrate temperature was 300 °C and the Ge cell temperature was 1325 °C for all samples.

Sample number	C cell current (A)	B cell temp. (°C)
SGC-261	49	1550
SGC-266	48.5	1550
SGC-267	49.5	1550
SGC-270	50	1550
SGC-102	0	1450
SGC-103	0	1650

absorption was not calibrated for possible optical scattering or leakage during the multiple reflections.

The absorption data were fit to the McFarlane–Roberts expression for band gap, E_g and phonon energy, E_{ph} above the band gap

$$\alpha = A \frac{(h\nu - E_g + E_{ph})^2}{e^{E_{ph}/kT} - 1}, \quad E_g - E_{ph} < h\nu < E_g + E_{ph},$$

$$\alpha = A \left[\frac{(h\nu - E_g - E_{ph})^2}{1 - e^{-E_{ph}/kT}} + \frac{(h\nu - E_g + E_{ph})^2}{e^{E_{ph}/kT} - 1} \right], \quad h\nu > E_g + E_{ph},$$

where $h\nu$ is the photon energy, E_g is the band gap, and E_{ph} is the phonon energy. Figure 2 shows the measured data and the MacFarlane–Roberts expression fit. Table II lists the measured optical band gaps for each of the samples. For our thick samples, the effect of alloying was to increase the band gap. For sample SGC-261, we observe a band gap of 772 meV, which is more than 100 meV greater than bulk Ge (664 eV). This large shift in band gap is useful for GeC/Ge heterostructures. We attribute the band gap difference to C incorporation, noting that diamond has a band gap of 5.45 eV. These layers are near fully relaxed, and thus the strain in these samples is small. Thus bulk strain reduction cannot account for all of the change in observed band gap. If we assume Vegard's Law, however, and attribute the entire shift in band gap to carbon incorporation, we infer C concentrations of $y \approx 0.02$. Since the relation between band gap and C fraction is not yet known, this linear method is not reliable for determining C concentration, especially for large C concentrations. It is known that the band gap of 3C-SiC ($E_g = 2.2$ eV) is much less than predicted by Vegard's Law ($E_g = 3.28$ eV) by interpolating between diamond and Si.

X-ray diffraction (XRD) measurements were performed to determine the structure, relaxation, and concentration of the films. The XRD measurements were performed on a

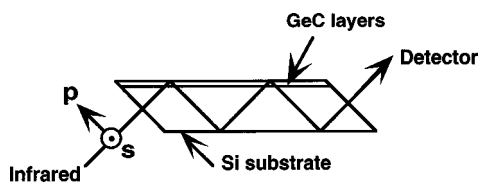


FIG. 1. Waveguide FTIR geometry for multiple bounces through the film. Electric polarization orientations (s and p) are indicated.

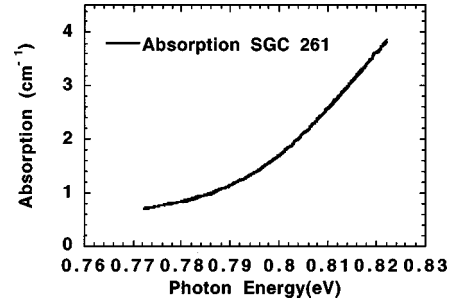


FIG. 2. FTIR absorption data for sample SGC-261 (thin line). The data are fit to the MacFarlane–Roberts expression above the band gap. Note how well the model (dark line) fits the data for an indirect band gap.

Philips X'Pert MRD materials research diffractometer using a $\text{CuK}\alpha$ radiation source. The $\text{CuK}\alpha$ radiation is selected by a four-bounce Ge (220) Bartels monochromator, and a triple-axis output monochromator for high resolution. The system is also equipped with a fully rotational rocking curve stage, which allows measurement of off-axis reflections. This allows the measurement of the d spacings and lattice parameters in the direction (a_{\perp}) of growth and in the plane of the substrate (a_{\parallel}). From these reflections, we can infer tilt, relaxation, and tetragonal distortion. Using the Poisson ratio, the bulk lattice parameter (a_0) can be inferred. In each case, the layer reflections are referenced to the Si substrate peak present in each scan. The substrate peak is corrected to the nominal value for Si ($a = 5.43088$ Å). Any correction in 2Θ to the measured Si peak is then applied to the 2Θ value of the layer peak. For the analysis in this article, the layers are assumed to exhibit only simple tetragonal strain, although there is the possibility of monoclinic or triclinic distortion.⁵ The specific nature of the strain of these layers was not meant to be addressed in this work.

Wide-range scans along the surface normal showed only (004) reflections from the layers, indicating the alloy layers have a structure highly oriented to the (100) substrate. The full width at half maximum (FWHM) values for the layers were on the order of tenths of a degree in 2Θ , indicating good quality layers. For this work, the (004), (113), and (224) + and - reflections were measured for each sample. The + and - designations refer to the opposite sample orientations in the diffraction plane, which, when averaged, give us the corrected scattering angle, 2Θ .⁶ Figure 3 shows the (004)+ scan of one of our samples. We calculate a_{\perp} from the average of the two (004) +/- reflections. We calculate a_{\parallel} from the (113) and (224) +/- reflections by first

TABLE II. Measured optical band gaps for the GeC layers.

Sample number	Optical band gap (meV)
SGC-261	772.18
SGC-266	766.66
SGC-267	763.13
SGC-270	766.31
bulk Ge	664.00

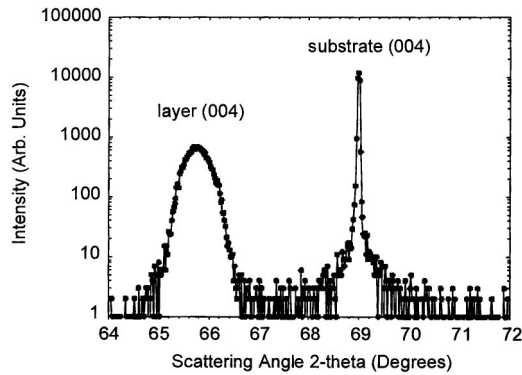


FIG. 3. XRD diffraction intensity vs diffraction angle of (004) layer/substrate reflection of sample SGC-261. The GeC layer peak appears around 65.8°, and the Si substrate peak occurs around 69°. Note the small width of the Si substrate peak, indicating a sharp system response.

using geometry to calculate the parallel lattice parameter for each reflection, and then averaging the four values.

The bulk lattice parameter (a_0) was also then calculated from a_{\perp} and a_{\parallel} as follows⁷:

$$a_0 = a_{\perp} + \frac{[2\nu(a_{\parallel} - a_{\perp})]}{1 + \nu},$$

where ν is the linear interpolated Poisson ratio for GeC from the values for Ge and C.⁸ The layer relaxation parameter, R , is then

$$R = \frac{a_{\parallel} - a_{\text{Si}}}{a_0 - a_{\text{Si}}},$$

where a_{Si} is the substrate lattice parameter.⁷ We assume Vegard's Law holds for the lattice parameter and back out an estimate for the C concentration (y). As references, we grew samples with no C [pure Ge on (100) Si], and then attributed the change in bulk lattice parameter in the alloys to the C. We then used the range of values obtained from the reference samples to obtain an average C concentration and error. The instrument error in XRD measurements is very small, especially with a high-resolution instrument. In addition, a near perfect peak fit using a Lorentzian or Pearson VII function

TABLE III. XRD data and calculations for the GeC layers.

Sample number	Bulk lattice parameter, a_0 (Å)	Relaxation (R)	Calculated carbon concentration
SGC-261	5.6482	0.9022	0.64% ± 0.16
SGC-266	5.6491	0.9155	0.59% ± 0.16
SGC-267	5.6571	0.9778	0.39% ± 0.16
SGC-270	5.6533	0.9439	0.21% ± 0.16
SGC-102	5.6582	0.9537	0% ^a
SGC-103	5.6650	0.9168	0% ^b

^aReference 1.

^bReference 2.

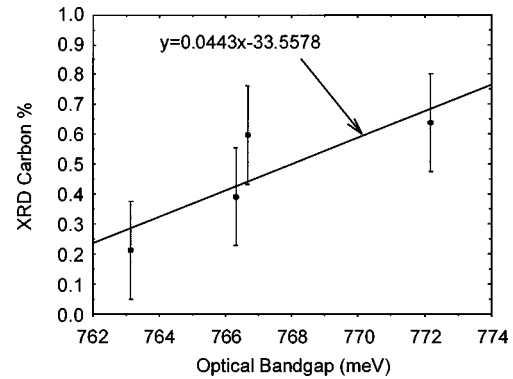


FIG. 4. Calculated carbon fraction vs FTIR measured optical band gap. The least-squares best-fit line is plotted. Note the clear trend of increasing band gap with carbon concentration.

(with confidence factor >0.95) is obtained for the measured XRD data.² Table III shows values for a_0 , relaxation, and the C concentration.

Comparing the FTIR band gap and XRD calculated C concentration yields an interesting result. Figure 4 shows a plot of band gap versus calculated C concentration. We find that C *increases* the optical band gap of Ge on Si. The least-squares best-fit line has been plotted on the graph as a convenience. We expect due to X and L maxima mixing, that the true relationship has some bowing. The best-fit line prediction of $E_g = 3.02$ eV underestimates the C diamond band gap ($E_g = 5.45$ eV).⁸ However, the trend of increased band gap with increasing C concentration is clear.

In conclusion, we have grown crystalline GeC alloys using low-temperature MBE. Measurements on the alloys layers show the incorporation of C increases the Ge band gap by more than 100 meV. XRD measurements confirm the crystalline structure of the samples and estimate C concentrations to be 0.2%–0.6%. These alloys offer a new material for use in Group IV heterostructures.

The authors gratefully acknowledge T. Tröger and T. Adam for useful discussion, and P. Thompson and K. Hobart for advice on MBE growth. This work was funded by the U.S. Army Research Office, Grant No. DAAH04-95-1-0625, and the Office of Naval Research, Grant No. N00014-93-1-0393.

¹H. J. Osten, B. Heinemann, D. Knoll, G. Lippert, and H. Rucker, *J. Vac. Sci. Technol. B* **16**, 1750 (1998).

²J. Kolodzey, P. A. O'Neil, S. Zhang, B. A. Orner, K. Roe, K. M. Unruh, C. P. Swann, M. M. Waite, and S. Ismat Shah, *Appl. Phys. Lett.* **67**, 1865 (1995).

³B. A. Orner, J. Olowolafe, K. Roe, J. Kolodzey, T. Laursen, J. W. Mayer, and J. Spear, *Appl. Phys. Lett.* **69**, 2557 (1996).

⁴S. Sauvage, P. Boucaud, F. H. Julien, J.-M. Gerard, and J.-Y. Marzin, *J. Appl. Phys.* **82**, 3396 (1997).

⁵W. J. Bartels, *J. Vac. Sci. Technol. B* **1**, 338 (1983).

⁶M. Fatemi and R. E. Stahlbush, *Appl. Phys. Lett.* **58**, 825 (1991).

⁷M. A. G. Halliwell, *Appl. Phys. A: Solids Surf.* **58**, 135 (1994).

⁸*Data in Science and Technology: Semiconductors, Group IV Elements and III-V Compounds*, edited by O. Madelung (Springer, Berlin, 1991).